Slow magnetic relaxations in the anisotropic Heisenberg chain compound Mn(III) tetra(*ortho*-fluorophenyl)porphyrin-tetracyanoethylene

M. Bałanda,[1] M. Rams,[2] S. K. Nayak,[3] Z. Tomkowicz,[2,*] W. Haase,[4] K. Tomala,[2] and J. V. Yakhmi[5]
[1]*H. Niewodniczański Institute of Nuclear Physics PAN, Radzikowskiego 152, 31-342 Kraków, Poland*
[2]*Institute of Physics, Jagiellonian University, Reymonta 4, 30-059 Kraków, Poland*
[3]*Bio-Organic Division, Bhabha Atomic Research Centre, Trombay, Mumbai 400 085, India*
[4]*Institut für Physikalische Chemie, Technische Universität Darmstadt, Petersenstrasse 20, 64287 Darmstadt, Germany*
[5]*Technical Physics & Prototype Engineering Division, Bhabha Atomic Research Centre, Mumbai 400 085, India*
(Received 25 June 2006; revised manuscript received 29 October 2006; published 18 December 2006)

Magnetic properties of manganese(III) tetra(*ortho*-fluorophenyl)porphyrin-tetracyanoethylene were studied by ac and dc measurements on polycrystalline samples. This compound consists of ferrimagnetic chains, in which magnetic moments of Mn ion ($S=2$) in the center of a porphyrin disc and of a tetracyanoethylene radical ($s=1/2$) are antiferromagnetically coupled with the exchange integral of $J=-217$ K. At low temperatures, slow magnetic relaxations (below 13 K) and irreversible magnetic behavior (below 4.5 K) were observed, which strongly resemble behavior of a single chain magnet, reported for Ising systems. Temperature dependence of the relaxation time is well described by the Arrhenius equation with the activation energy $\Delta E=117$ K. These relaxations are interpreted as a thermally activated reversal of magnetization through the energy barrier ΔE, associated with creation and propagation of domain walls in one-dimensional anisotropic Heisenberg systems.

DOI: 10.1103/PhysRevB.74.224421 PACS number(s): 75.50.Xx, 75.10.Pq, 75.40.Gb, 75.60.Ch

I. INTRODUCTION

Molecular magnetism is a dynamically developing field of science with prospects for applications. Recently, so-called single molecule magnets[1] (SMM) and single chain magnets[2–4] (SCM) have been objects of interest. SMM materials are composed of molecules with a high spin and strong easy axis anisotropy. Each such molecule can function as a magnet at temperatures below its superparamagnetic blocking temperature. Due to this property, SMM can be used to build the ultimate high-density memory. Therefore, considerable efforts are devoted to the search for new materials with similar properties but with higher blocking temperatures. The interest in SCM is a natural consequence in this field. The number of SCM reported to date is not large. These materials are composed of ferro- or ferrimagnetic chains, which are well isolated Ising systems. Only recently, one SCM was reported, chains of which are anisotropic Heisenberg systems.[5] In our previous studies[6,7] we synthesized manganese porphyrin-radical polymers with alcoxy substitutions having very high interchain distance up to 30 Å. Such materials are good candidates for SCM. Unexpectedly, a phase transition to the state with spontaneous magnetization was observed. A theoretical model explaining this phase transition takes into account superspin interactions and a strong single ion anisotropy.[8]

The family of metalloporphyrin-tetracyanoethylene based magnets provides an unusual opportunity for magnetic studies, due to the relative ease of modifying the structure through, e.g., various substitutions at the porphyrin disc periphery. In this way, magnetic dimensionality can be varied by increasing the interchain separation. Molecular structure of manganese tetraphenylporphyrin-tetracyanoethylene, [MnT*X*PP][TCNE], where X (=R or R') is a substituent, is shown in Fig. 1. In the center of the porphyrin disc the Mn^{III} ion is located, which forms the chemical bond with the TCNE radical.

The spin of the Mn^{III} ion $S=2$ is strongly antiferromagnetically coupled with a delocalized spin $s=\frac{1}{2}$ of the TCNE radical. The constant of the exchange coupling for some of these compounds is of the order of 100 cm^{-1}.[9]

Although the family of metalloporphyrin-radical magnets offers a wide range of magnetic behavior, there is some common property of nearly all representatives—partially, or even fully spin glass—or superparamagneticlike character of these substances.[10–12] It is known[11] that a disorder may come from solvent molecules, which are present in free space between chains, as well as from some freedom in orientation of the bridging TCNE molecule. We reported the partially glassy character of [MnT*X*PP][TCNE]·solvent, X=alcoxy.[7,13] As suggested, this glassiness was caused by the presence of frustrated clusters of segments of chains coupled by dipolar interactions.[13] It was observed that with increasing magnetic field, the behavior gradually became superparamagnetic or SCM-like, as if the field decoupled the chains (field symmetry incompatible with dipolar coupling).

Gîrţu *et al.*[14,15] suggested that the cluster glasslike behavior observed for the two manganese porphyrin-TCNE compounds with different solvents: [MnTPP][TCNE]·y(*o*-xylene) and [MnTPP][TCNE]·y(*o*-dichlorobenzene) is caused by disorder leading to the origin of one-dimensional clusters coupled through dipole-dipole interactions to form three-dimensional domains. Etzkorn *et al.*[16] studied spin glass transition for [MnTPP][TCNE]·2(1,3-$C_6H_4Cl_2$), which occurs near 4 K and proposed a quasi-1D fractal cluster glass model describing magnetic viscous behavior of this transition. The dimension D of spin clusters was determined to be in the range 0.8–1.5. As temperature was lowered, D became greater than 1, meaning that clusters included portions of neighboring chains.

The origin of glassiness in these compounds is intriguing because compounds are one-dimensional anisotropic systems with strong intrachain coupling. It is not apparent how the

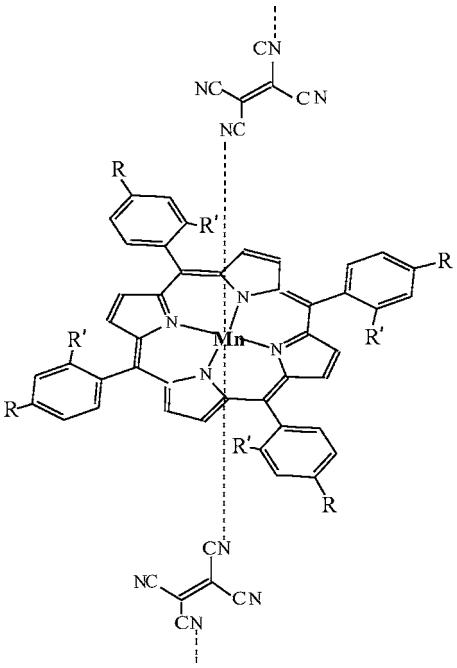

FIG. 1. Molecular structure of (MnT*X*PP)(TCNE). Two positions: *R* (*para*) and *R'* (*ortho*) for *X* substitutions are shown.

crystallographic disorder introduces magnetic disorder and how magnetic frustration appears. Thus, more studies are needed on similar compounds in order to shed light on the nature of this glassiness.

The subject of this paper is the [MnT*R'*PP][TCNE] compound with $R'=$F. The substances of the composition [MnT*X*PP][TCNE] were synthesized by Miller's group with the *X* atom substituted in the *para*- ($X=$F,Cl,Br,I),[17–19] as well as in the *ortho*-position ($X=$F'),[20] see Fig. 1. It was found[19] that [MnTFPP][TCNE] compound (with F in *para* position) undergoes a phase transition to a magnetically ordered state with a critical temperature $T_c \sim 28$ K. The low temperature behavior of the [MnTF'PP][TCNE] compound (F in ortho position) was suggested to be of a spin glass or of superparamagnetic character.[20] The polycrystalline samples of [MnTF'PP][TCNE] obtained by us showed superparamagnetic or SCM-like relaxations. It was surprising because the interchain distance in this compound, which is ~11 Å, is considerably shorter than for the above mentioned compounds with alcoxy substitutions[9] and a magnetic phase transition was rather expected.

Below we present results of ac and dc magnetic measurements performed for polycrystalline [MnTF'PP][TCNE]·*x* toluene. The aim is to learn the nature of magnetic relaxations.

II. EXPERIMENTAL

A. Synthesis

Meso-tetrakis(*ortho*fluorophenyl)porphyrin was prepared from pyrrole and *ortho*-fluorobenzaldehyde utilizing a literature method.[21] Manganese(III) tetrakis (*ortho*fluorophenyl)porphyrin chloride was prepared from meso-tetrakis(*ortho*fluorophenyl)porphyrin and $Mn(OAc)_2 4H_2O$ using dimethylformamide (DMF) as solvent, followed by acidification with 6*N* aqueous HCl which was further reduced by $NaBH_4$ in CH_3OH/pyridine mixture to manganese(II) tetrakis(*ortho*fluorophenyl)porphyrin as the pyridine adduct, following the method described in the literature.[22] Finally, keeping a mixture of manganese(II) tetrakis(*ortho*fluorophenyl)porphyrin and tetracyanoethylene (TCNE) in toluene (PhMe) at room temperature yielded a dark green precipitate. The solid was filtered off and dried under vacuum to furnish manganese (III) tetrakis-(*ortho*fluorophenyl)porphyrin tetracyanoethenide salt [MnTFPP][TCNE]·*x*PhMe ($x \sim 2$) in 65% yield.

It was checked that the samples were stable during several months when kept in a refrigerator in closed ampoules.

B. Methods of investigation

Infrared absorption spectrum was recorded with a Perkin Elmer FT-IR 1000 PC spectrometer. The sample for this study was mixed with Nujol. X-ray diffraction was performed with CuKα radiation by means of a DRON diffractometer using Debye-Scherrer geometry.

ac magnetic susceptibility χ_{ac} was measured using a Lake Shore 7225 susceptometer. Measurements of both components of $\chi_{ac}=\chi'-i\chi''$ were carried out as a function of temperature, frequency f and oscillating field amplitude H_{ac} in zero as well as nonzero superimposed static magnetic field. Higher harmonics χ_2 and χ_3 of the fundamental susceptibility were also measured. DC magnetization data were obtained with a Quantum Design magnetometer, model MPMS 5XL. In the zero field cooling (ZFC) regime, the sample was cooled in zero magnetic field, then the field was switched on and magnetization was measured on heating in this field. In field cooling (FC) regime, the sample was cooled in field and subsequently measured in this field on heating. The obtained data were corrected for the core diamagnetic contribution.

The polycrystalline samples used for magnetic studies were pressed into pellets. This was necessary as in other cases irreproducible results were obtained because magnetically anisotropic grains could rotate in response to magnetic field.

The material was inspected with a Hitachi S-4700 scanning electron microscope (SEM), having the maximum resolution of 2 nm. For observation, the crystallites, scattered on a foil, were evaporated with a thin layer of graphite.

III. RESULTS

A. Structural and morphological characterization

Infrared absorption spectrum was taken to confirm the success of the bridging reaction. The characteristic infrared stretching frequencies ν_{CN} were 2144 and 2194 cm^{-1}. These values are consistent with the presence of $[TCNE]^{\bullet -}$ as indicated by the large shifts to lower energy from 2259 and 2221 cm^{-1} for neutral TCNE.[19]

The x-ray powder diffraction pattern, obtained at 300 K, is shown in Fig. 2. The pattern is compared with the Rietveld fitted profile,[23] based on the structural data of Brandon *et*

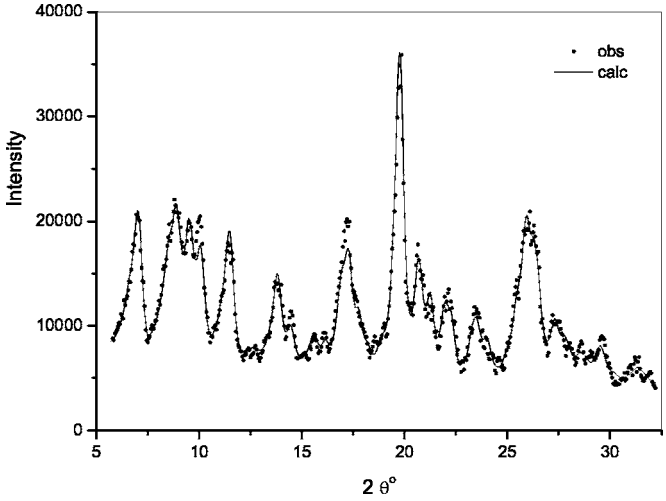

FIG. 2. X-ray diffraction pattern compared with the profile calculated using crystallographic data from Ref. 20.

al.,[20] obtained at 77 K. As seen, there is qualitative agreement between observed and calculated patterns. Some discrepancies may result from the fact that only profile parameters were fitted but structural ones were fixed.

On the SEM images, one of which is shown in Fig. 3, the grains of different dimensions 50–500 μm were observed. Large magnifications were used in order to see nanoparticles, but their presence could not be confirmed.

B. ac measurements

The temperature dependence of ac susceptibility measured at various frequencies and by the amplitude $H_{ac}=2$ Oe are shown in Fig. 4. No higher harmonics χ_2 and χ_3 of the fundamental susceptibility were observed, even at $H_{ac}=10$ Oe. The absence of χ_2 in zero dc magnetic field means that the sample has no spontaneous magnetic moment. The absence of the χ_3 signal means that no spin glass transition occurs.

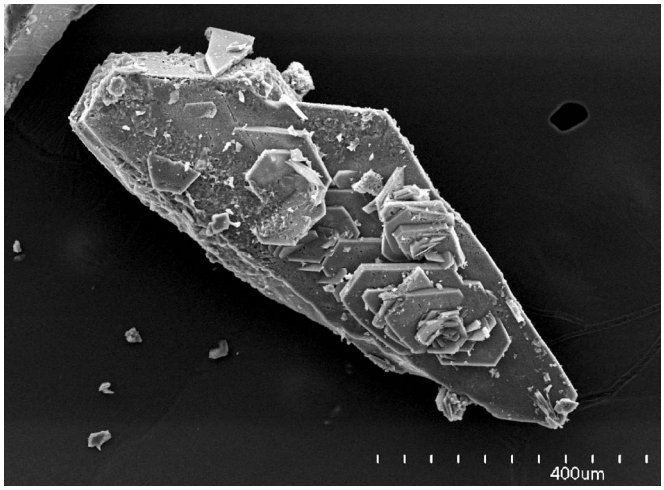

FIG. 3. SEM image of one of the greatest grains of the $[Mn^{III}TF'PP]$ [TCNE] compound. The grain is overgrown with smaller crystallites.

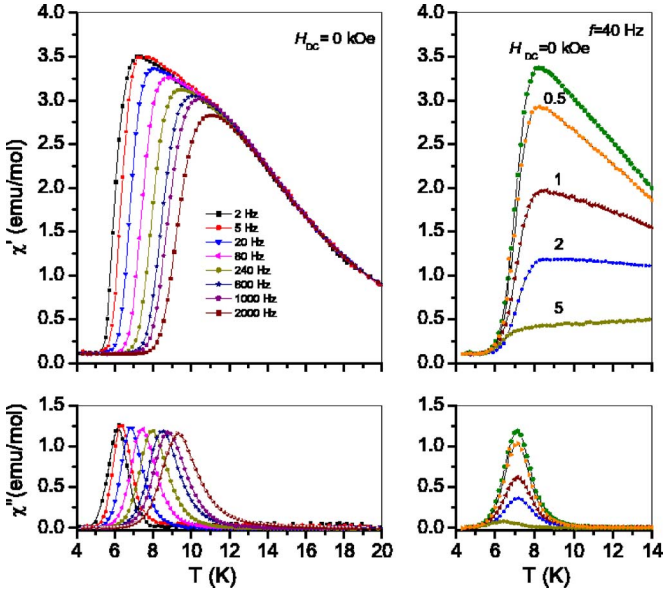

FIG. 4. (Color online) Temperature dependence of ac susceptibility obtained for different frequencies at $H_{dc}=0$ Oe (left panel) and for different superimposed static magnetic fields at the frequency of 40 Hz (right panel). The amplitude of the driving magnetic field is $H_{ac}=2$ Oe.

As seen in Fig. 4, χ' first increases with decreasing temperature, reaches a maximum and falls down to a small value of ~0.09 emu/mol. Close behind this maximum the accompanying χ'' peak appears. The right panel shows the dependence on superimposed dc magnetic field, which strongly suppresses both χ' and χ'' components. The dependence on frequency is shown in the left panel. It is seen that the χ'' peak moves as a whole with frequency. The relative variation of the χ'' peak temperature T_p per decade change of frequency is $\Delta T_p/(T_p \Delta \log f)=0.13$. This value is above the typical limits 0.004–0.08 observed for traditional spin glasses[24] and is characteristic for cluster glasses, superparamagnets, or SCM. From the frequency shift, a temperature dependence of the relaxation time τ can be obtained, assuming $\tau=1/2\pi f$ at $T=T_p$. This frequency shift could be well fitted with the Arrhenius equation

$$\tau = \tau_0 e^{E_a/kT}, \tag{1}$$

where E_a is the activation energy and τ_0 the characteristic microscopic time. The values of parameters obtained from the fit were $E_a=117\pm5$ K, $\tau_0=(1.4\pm0.5)10^{-10}$ s. Reciprocal temperature dependence of τ is shown in Fig. 5 in the logarithmic scale together with data obtained from dc measurements (see the next section). The solid line is a fit through the dc data; as seen it agrees with the ac data. The parameters obtained from this fit are $E_a=112\pm2$ K, $\tau_0=(4.4\pm0.5)10^{-10}$ s.

Having in mind different interpretation of similar results,[16] the ac data were also analyzed using equations of other (non-Arrhenius) activated dynamics, as well as the equation for the normal critical slowing down, taking place by approaching some critical temperature. All ac data, obtained with and without superimposed static magnetic field,

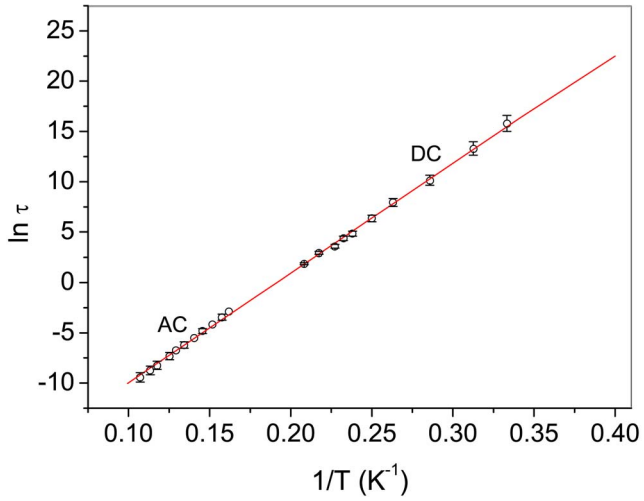

FIG. 5. (Color online) Reciprocal temperature dependence of the relaxation time. Experimental points were obtained from the frequency dependent ac susceptibility and from dc magnetization relaxation measurements (see the next section). The solid line is a linear fit to dc data.

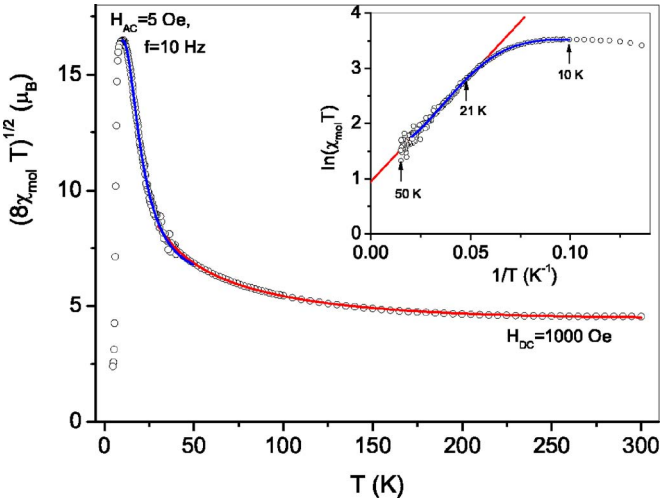

FIG. 7. (Color online) Temperature dependence of $(8\chi_{mol}T)^{1/2}$ for [MnTF′PP][TCNE]. High temperature data ($T>37$ K) are dc data, obtained in the field of 1000 Oe. Below 37 K, ac data are shown. Inset: reciprocal temperature dependence of $\ln(\chi_{\mathrm{mol}}T)$–ac data only. Solid lines are fits (see text).

were taken into account. The evolution of parameters in equations with increasing magnetic field was watched. However, the most consistent results were obtained by analyzing the data with the Arrhenius equation, which points to the absence of phase transition at $T>0$ K. The presence of phase transition cannot be fully excluded, but its critical temperature is certainly below 2 K.

ac data, obtained under static superimposed magnetic field, were used to obtain the field dependence of the activation energy E_a. This dependence is shown in Fig. 6. As seen, E_a decreases with increasing field. Because dc field suppresses ac susceptibility, the determination of E_a for fields greater than 7 kOe was not possible.

ac data were also used to obtain the distribution of relaxation times. This distribution was determined from χ'' vs χ' Argand plots (not shown). The plots deviated a little from semicircles, being circular arcs of size $(1-\alpha)\pi$ with $\alpha=0.12\pm0.02$. This means that the distribution of relaxation times is small and nearly does not change with temperature in the range 6–9 K. It is worth mentioning that for typical spin glasses, rather high values of α (~0.8; Ref. 25) and its strong temperature dependence are expected. Small and temperature independent values of α are characteristic for superparamagnets and SCM ($\alpha\sim0.1$; Refs. 25 and 26). However, it should be noted, that the temperature range, where these relaxations were observed, is rather narrow. Indeed, a considerable distribution of relaxation times was observed in dc study, i.e. at lower temperature range; see the next section.

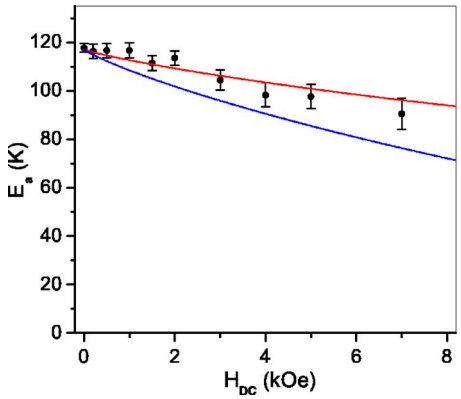

FIG. 6. (Color online) Activation energy of the Arrhenius equation for the relaxation time determined as a function of superimposed dc magnetic field. The solid lines are calculated dependences; see Discussion.

C. dc measurements

In this section, results of magnetization measurements are presented. The measurements were performed as a function of temperature, magnetic field and time.

Figure 7 shows the temperature dependence of the product $\chi_{mol}T$ represented through the quantity $(8\chi_{mol}T)^{1/2}$. Such form of presentation is popular in magnetochemistry, where this quantity is called the effective magnetic moment. Its high temperature limit is the paramagnetic moment of a molecule expressed in μ_B. The data in Fig. 7 are composed from two sets. Only the high temperature data (above 37 K) are dc data. At low temperature range, the dc data were substituted by ac data, which do not differ much, but the maximum at $T\sim10$ K is higher. In this way the data in Fig. 7 can be treated as the "true" zero field data. The maximum at $T\sim10$ K is also shown in the insets to Fig. 7 and Fig. 8. The room temperature value of $(8\chi_{mol}T)^{1/2}$ is somewhat lower than the expected high temperature limit of 5.2 μ_B (calculated assuming $S=2$, $s=1/2$, $g_S=g_s=2$). This is understandable when the minimum of $(8\chi_{mol}T)^{1/2}$ (expected for one-dimensional ferrimagnet) occurs just near room temperature.

The temperature dependence of $(8\chi_{mol}T)^{1/2}$ was fitted with the expression derived by Seiden[27] for an infinite linear magnetic system with alternating quantum spin $s=\frac{1}{2}$ and classical

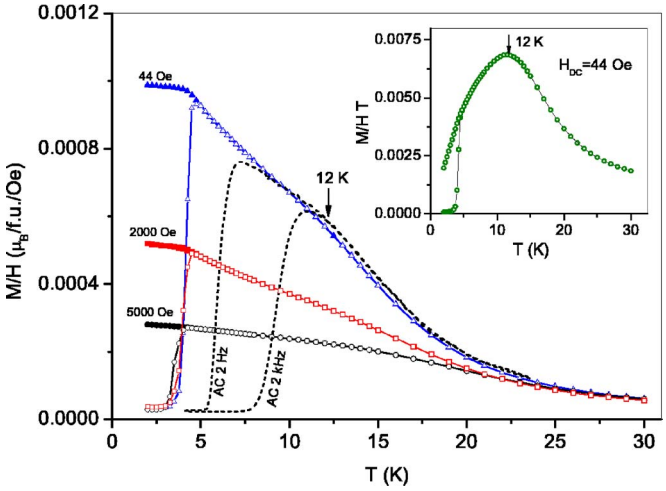

FIG. 8. (Color online) FC (full symbols) and ZFC magnetization (open symbols) vs temperature plots for [MnTF′PP][TCNE]. For comparison, two ac susceptibility $\chi'(T)$ curves were included (H_{ac}=2 Oe). Inset: temperature dependence of the MT/H product.

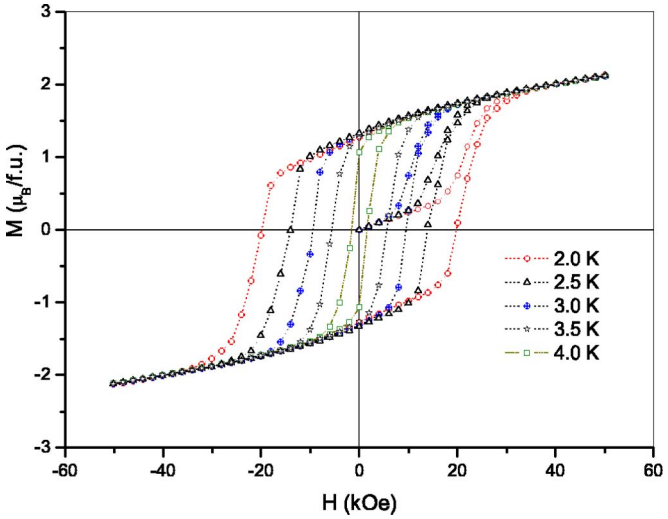

FIG. 9. (Color online) Magnetic hysteresis loops measured at different temperatures.

spin S=2 coupled by the isotropic exchange according to the Hamiltonian

$$H = -J\sum_i (S_i + S_{i+1})s_i. \tag{2}$$

In the fit, a small correction for a temperature independent paramagnetism was taken into account. Good agreement with the isotropic Heisenberg model was obtained in the temperature region 32–300 K, in which no field dependence was observed (see Fig. 8). The fit is shown in Fig. 7. The exchange constant obtained from the fit is J=−217 K. The uncertainty of J can be estimated to be ±10 K and results mainly from the uncertainty of the fitting region. Below the fitting region, the fit goes under the experimental curve. It is expected that at low temperatures, the magnetic behavior of the 1D system is better described by the anisotropic Heisenberg model, which, in the limit of zero field, predicts the following (Ising-like) temperature dependence of the parallel susceptibility[28]

$$\chi T \propto e^{\Delta_\xi/kT}, \tag{3}$$

where Δ_ξ is the creation energy of the domain wall in the chain (the low temperature perpendicular susceptibility is lower and less dependent on temperature). If this model is pertinent here, the experimental quantity ln (χT) should be a linear function of $1/T$. In the inset to Fig. 7, the reciprocal temperature dependence of ln($\chi_{mol}T$) is shown. All these data come from ac measurements. As seen, a part of the dependence can be well approximated by a straight line, however, at lower temperatures the experimental points diverge from the straight line, which can be explained by a finite length of chains. Also a small antiferromagnetic interaction can come into play because ln($\chi_{mol}T$) slightly decreases below 10 K (see also the inset to Fig. 8). By fitting the low temperature dependence in Fig. 7, the finite length (according to Refs. 29 and 30) and antiferromagnetic interaction J' in the molecular field approximation were taken into account. Excellent fit was obtained in the range 35–10 K (see inset) and even below. The parameters obtained from fit are Δ_ξ=60 ±3 K, zJ'=−0.12 K, and n=50 ±4, where n is a number of links (S, s), z is a number of neighbor chains. The proportionality constant in Eq. (3), obtained from fit, is 1.04 ±0.12 emu K/mol in good agreement with the predicted value (1.125) for the resultant spin S_T=3/2. As seen, the antiferromagnetic interaction is weak; the relative strength of inter- to intrachain interaction is $zJ'/J \sim 6\times 10^{-4}$.

In Fig. 8, FC magnetization M_{FC} and ZFC magnetization M_{ZFC} are presented, as quantities normalized to dc magnetic susceptibility. These quantities were measured as a function of temperature in various dc magnetic fields of strength from 44 up to 7500 Oe (not all results are shown, for better clarity).

As seen, M_{FC}/H and M_{ZFC}/H curves strongly diverge at the bifurcation point, which is about 4.5 K at low fields, but moves to lower temperatures with increasing field. M_{FC}/H has plateau at low temperatures and M_{ZFC}/H values become small, similarly as for ac susceptibility curves, which are also shown in the figure.

The field dependence of magnetization, obtained in the form of hysteresis loops at several different temperatures, is shown in Fig. 9. The hysteresis loops appear below the bifurcation point. No hysteresis was observed at 2 K when measurement was limited to the field range ±10 kOe. The sweep rate of the field during all these measurements was typically 100 s per point.

Next, time dependences of the thermoremanent magnetization (TRM) were measured at different temperatures. In this experiment, the sample was cooled with a rate 1 K/min in a field of 1000 Oe to the given temperature, kept at this temperature 5 min (waiting time). Next, the field was off and the time measurement started. The results are shown in Fig. 10. All experimental curves could be well-fitted using the stretched exponential form

$$M(t) = \sigma_0 + M_0 \exp[-(t/\tau)^{1-n}], \tag{4}$$

where τ is the mean relaxation time and $0 \leqslant n \leqslant 1$; a larger n corresponds to a broader distribution of relaxation times. The

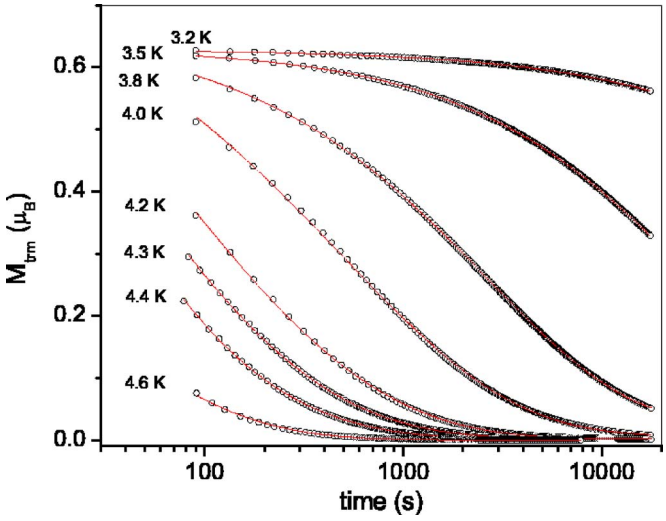

FIG. 10. (Color online) Thermoremanent magnetization vs time dependence obtained for different temperatures. Solid lines are fits to the stretched exponential.

additive constant σ_0 was necessary to obtain good fits. The fitted values of τ varied systematically from 6.5 to 6 $\times 10^6$ s through the temperature range 4.8–3 K. The distribution of relaxation times is notable because the obtained values of the n parameter oscillated about 0.5. Results for τ are shown in Fig. 5 in the form of $\ln(\tau)$ vs reciprocal temperature dependence together with the values of τ obtained from ac measurements.

For spin glasses, the relaxation time depends on the waiting time (so-called ageing effect). We checked this dependence for $T=3.8$ K. In one case, the waiting time was 5 min, in the second case it was 60 min, but no difference in relaxation time was observed, confirming the non-spin-glass character of the studied compound.

Measurements of time dependence were also performed at 2 K when magnetic field of various intensities was applied antiparallel to the initial magnetization direction. The aim

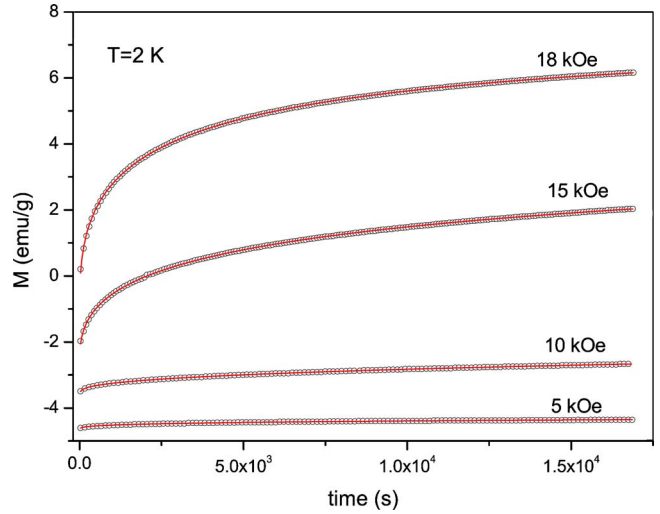

FIG. 11. (Color online) Magnetization relaxation (at $T=2$ K) following switching magnetic field from −50 kOe to various values given in the figure. Solid lines are fits to the stretched exponential.

was to create conditions typical for experiments on magnetization switching in nanosized Ni wires.[31] Experimental results, shown in Fig. 11, were fitted with Eq. (4). From the fits, relaxation times were obtained. While the relaxation time for $H<5$ kOe is immeasurably long, it drastically decreases with increasing field. Here, the value of the parameter n is also about 0.5.

IV. DISCUSSION

The magnetic behavior of [MnTF′PP][TCNE]·x toluene is very similar to that observed for the single chain magnet (SCM). Most SCMs, known up to date, are linear Ising systems. Slow magnetic relaxations in such systems were predicted theoretically by Glauber.[32] The 1D ferrimagnet [MnTF′PP][TCNE]·x toluene with its high value of J, equal to −217 K, is an anisotropic Heisenberg system, because single ion easy axis anisotropy parameter D of the Mn^{III}-ion is small as compared to J. The value of D can be estimated from EPR and susceptibility measurements on single molecules of manganese tetraphenyl porphyrin, axially ligated by one or two (different) ligands. The D values in the limits of 2.1–4.3 K were obtained depending on ligands.[33,34] The easy axis direction was found to be perpendicular to the molecule plane. Unfortunately, there is no D data for molecules with two N ligands. In such low anisotropy systems, relaxations occur by excitations of broad domain walls, which are solitary waves. This is in contrast to Ising systems, where domain walls are extremely narrow.

In general, there can be different soliton excitations: single domain wall excitations, which are π solitons, and paired domain walls, which are soliton-soliton pairs (so called 2π solitons with the same twist of two domain walls) or soliton-antisoliton pairs (with the opposite twist). In short chains, π solitons are present. With increasing length of chains, the excitation probability of paired solitons increases.[35]

The creation energy of solitons in a ferromagnetic chain of equal spins S in zero magnetic field is[36]

$$\Delta E = 2k\sqrt{2JSSDSS}. \tag{5}$$

The factor k equals 1 or 2, depending on whether solitons are singled ($k=1$) or paired ($k=2$). In nonzero magnetic field, soliton-antisoliton pairs are created with greater probability because their creation energy decreases with field. The field dependence is given by the factor $(\tanh R - hR)$, where $R=\operatorname{arcosh}(\sqrt{1/h})$, and $h=g\mu_B HS/(2DS^2)$, g=2.[35,37] This factor equals 1 for $H=0$. Equation (5), modified for the case of the ferrimagnetic chain composed of different spins S and s being in field, is

$$\Delta E = 2k\sqrt{|J|SsDS^2}(\tanh R - hR), \tag{6}$$

with $h=g\mu_B H(S-s)/2DS^2$. It has been taken into account that only the Mn ion has single ion anisotropy.

The value of activation energy E_a (117 K, obtained from ac measurements) is about two times greater than the creation energy of domain walls Δ_ξ (60 K, obtained from the fit in Fig. 7), which, at first glance, suggests 2π solitons. How-

ever, as we have shown, the length of chains is rather small, about 50 links (~500 Å) and in the temperature range where relaxation times were measured (below 9 K, see inset to Fig. 7), we are already at the finite length regime, in which correlation length is greater than the chain length. Thus, only π solitons are expected and they are excited at the chain ends. According to Refs. 5 and 30, E_a is always greater than Δ_ξ by some quantity Δ_A, i.e., $E_a=\Delta_A+\Delta_\xi$. Here, Δ_A equals 57 K. The quantity Δ_A is interpreted as an energy barrier of the characteristic time τ_0 [prefactor in Eq. (1)], which describes dynamics of the moving domain wall. For Ising systems, which have narrow domain walls, Δ_A equals DS^2. For anisotropic Heisenberg systems, Δ_A is expected to be greater. Equating ΔE of Eq. (6) (at $H=0$) and Δ_ξ we can estimate the value of D. Substituting $J=-217$ K and $k=1$, we obtain $D=1.04$ K. Also, the domain wall width W can be estimated from the equation $W=2\sqrt{Js/(DS)}a$, where a is the intrachain interspin distance. Taking $a=5.1$ Å ($S-s$ distance), the value $W\cong 75$ Å is obtained. Because the obtained value of D is too low, the value of W is too large. However, it should be noted that Eqs. (5) and (6) are not expected to be exact because they were derived for classical spins in the continuum approximation.

Let us see how the obtained picture with π solitons is consistent with other experimental data. First, as already shown (see Fig. 4), the χ'' component of ac susceptibility of [MnTF′PP][TCNE]·x toluene disappears quickly with increasing strength of superimposed magnetic field. This is understood taking into account the saturation effect and that the π solitons are suppressed by increasing field.[38] Second, as follows from Eq. (6), the creation energy of soliton decreases in field. The comparison of the experimentally found $E_a(H_{dc})$ dependence with the calculated field dependence of $\Delta_A+\Delta E$ is given in Fig. 6. The latter was calculated assuming that Δ_A (i) does not depend on the magnetic field (upper curve), and that (ii) depends in the same way as ΔE (lower curve). As seen, a better agreement with experimental data is obtained for the case (i). However, it is not a firm conclusion because the experimental value of the D parameter is not exactly known.

Relaxations observed in dc experiments in zero static magnetic field (see Fig. 10) can also be explained with π solitons. In this case, magnetization decays due to thermal excitations and propagation of domains walls. This is expected, because, as known, the one-dimensional system can not order at a finite temperature.

For very long chains and higher fields, another soliton mechanism becomes energetically favorable even for finite chains.[35,39] According to this mechanism, domains are nucleated, the walls of which are bound pairs of soliton and antisoliton. At sufficiently strong magnetic field, relaxations abruptly speed up because of multiple nucleation and instability of solitons. This occurs when many domains with critical size grow and join each other.[35] The activation energy becomes two times lower. The abrupt reversal of magnetization, like a switching, can be observed for this case, as reported for nanosized Ni wires.[31] It seems that the reversal of magnetization for our substance near H_c has such character. It is worthwhile to note here that the change of magnetization by reversal at H_c would be 6 μ_B with H parallel to easy axis. However, for the polycrystalline sample, the expected value is only 1/3 of this value. In fact, the change ~2 μ_B is observed. The other 2/3 of crystallites should show reversible behavior with the saturation value ±3 μ_B, which is not attainable at 50 kOe because of anisotropy.

We measured relaxation times when field was applied in the direction antiparallel to the initial magnetization direction (see Fig. 11). For such a case, there is a possibility to estimate relaxation times using Eq. (8) of Ref. 35. The calculated times for magnetization reversal obtained from this equation (assuming the damping constant $\alpha=0.01$) appeared to be several orders shorter than the observed ones. The reason can be that the model presented in Ref. 35 does not predict the appearance of quantity Δ_A and that the pinning can play a role in slowing relaxations down. The pinning forces originate because of defects, as reoriented TCNE molecules, solvents, also rotations of phenyl groups, which distort the porphyrin molecule[40] and influence locally J and D values, but also from inhomogeneity of interchain interactions. The latter results from a distribution in the length of the correlated chain segments, which are randomly distributed in adjacent chains. At sufficiently low temperature or by approaching a phase transition, the soliton motion is gradually blocked. For [MnTF′PP][TCNE]·x toluene at 2 K and small magnetic fields, the domain motion is completely frozen. Therefore, no hysteresis loop at 2 K was observed in fields below 10 kOe.

We would like to recall some reports on relaxations in similar systems. Evangelisti *et al.*[41] studied relaxations in ferromagnetic porphyrin chains of α-iron(II) phthalocyanine. This substance had no intermediary molecule (like TCNE) in the chain between porphyrin discs and the chains were classified as Ising systems. The relaxations were interpreted as π solitons. The authors suggested pinning of solitons to explain the slowing down of relaxations. Elmassalami *et al.*[42] observed simultaneously single and paired solitons in doped ferromagnetic Ising chain systems. Using the NMR method, Ferraro *et al.*[43] studied the chain compound $Mn(hfac)_2NITiPr$, which is a one-dimensional ferrimagnet formed by Mn(II), $S=5/2$ and nitronyl-nitroxide NITiPr, $s=1/2$. Here magnetic chains are weakly anisotropic Heisenberg systems with J value equal to 460 K and $D\cong 0.3$ K. The characteristics, typical for SCM, such as hysteresis, were not reported. The relaxations, observed in magnetic field, were rather quick and explained assuming paired solitons. Other examples are given in Ref. 30.

Although we confirmed that the sample is not a spin glass, there is some randomness, which can be caused by defects (see Introduction), likely being also the reason of the finite chains. Because the stretched exponential function had to be used to describe the time dependence of magnetization, it means that a distribution of relaxation times at low temperatures takes place. This can be also due to the increasing strength of antiferromagnetic interchain interactions as well as to different orientations of grains in the polycrystalline sample.

V. CONCLUDING REMARKS

The object of investigations was the ferrimagnetic chain compound manganese(III) tetra(*ortho*-

fluorophenyl)porphyrin-tetracyanoethylene, the magnetic properties of which were studied by ac and dc techniques. Although no sign of a magnetic phase transition was observed, the compound shows hysteresis loop below 5 K with the coercive field of 20 kOe at 2 K. At higher temperatures, up to 13 K, slow magnetic relaxations were observed, similar to the ones observed for single chain magnets. For the description of magnetic properties, an anisotropic Heisenberg model was adopted. Intrachain exchange coupling was determined to be $J=-217$ K. Temperature dependence of the relaxation time obeys the Arrhenius equation with an activation energy of 117 K, related to the excitation energy of the domain walls. Abrupt change of magnetization near the coercive field resembles a switching of magnetization, which was reported in the literature for Ni nanowires.

No typical glassy properties were observed. Earlier reported glasslike character of some Mn porphyrin-radical chain compounds may also be due to solitons.

ACKNOWLEDGMENTS

Thanks are due to R. Clérac (Centre de Recherche Paul Pascal, France) for helpful discussion. We also thank J. Faber for making SEM images using the microscope of the Laboratory of Electron Microscopy and Microanalysis at the Institute of Geological Sciences of Jagiellonian University. W.H., M.B., S.K.N., J.V.Y., and Z.T. thank Internationales Buero des BMBF for financial support.

*Corresponding author. Email address: z.tomkowicz@uj.edu.pl.

[1] L. Thomas, F. Lionti, R. Ballou, D. Gatteschi, R. Sessoli, and B. Barbara, Nature (London) **383**, 145 (1996).

[2] A. Caneschi, D. Gatteschi, N. Lalioti, C. Sangregorio, R. Sessoli, G. Venturi, A. Vindigni, A. Rettori, M. G. Pini, and M. A. Novak, Angew. Chem. **113**, 1810 (2001); A. Caneschi, D. Gatteschi, N. Lalioti, C. Sangregorio, R. Sessoli, G. Venturi, A. Vindigni, A. Rettori, M. G. Pini, and M. A. Novak, Europhys. Lett. **58**, 771 (2002).

[3] R. Clérac, H. Miyasaka, M. Yamashita, and C. Coulon, J. Am. Chem. Soc. **124**, 12837 (2002).

[4] H.-Z. Kou, Z.-H. Ni, IXth International Conference on Molecule-based Magnets (ICMM2004), Tsukuba, Japan, October 4–8, 2004, Abstract PA-077 (unpublished); T. Kajiwara, M. Nakano, A. Igashira-Kamiyama, and T. Ito, *ibid.*, PA-079; J.-L. Zuo, S. Wang, S. Gao, Y. Song, and X.-Z. You, *ibid.*, B-009; M. Ferbinteanu, H. Miyasaka, W. Wernsdorfer, K. Nakata, K. Sugiura, M. Yamashita, C. Coulon, and R. Clérac, J. Am. Chem. Soc. **127**, 3099 (2005).

[5] H. Miyasaka, T. Madanbashi, K. Sugimoto, Y. Nakazawa, W. Wernsdorfer, K. Sugiura, M. Yamashita, C. Coulon, and R. Clérac, Chem.-Eur. J. **12**, 7021 (2006).

[6] K. Griesar, M. A. Athanassopoulou, E. A. Soto Bustamante, Z. Tomkowicz, A. J. Zaleski, and W. Haase, Adv. Mater. (Weinheim, Ger.) **9**, 45 (1997).

[7] M. Bałanda, K. Falk, K. Griesar, Z. Tomkowicz, and W. Haase, J. Magn. Magn. Mater. **205**, 14 (1999).

[8] S. Ostrovsky, W. Haase, M. Drillon, and P. Panissod, Phys. Rev. B **64**, 134418 (2001).

[9] K. Falk, Ph.D. thesis, Darmstadt University, 2002.

[10] W. Hibbs, D. K. Rittenberg, K.-I. Sugiura, B. M. Burkhart, B. G. Morin, A. M. Arif, L. Liable-Sands, A. L. Rheingold, M. Sundaralingam, A. J. Epstein, and Joel S. Miller, Inorg. Chem. **40**, 1915 (2001).

[11] M. A Gîrțu, C. M. Wynn, K.-I. Sugiura, Joel S. Miller, and A. J. Epstein, Synth. Met. **85**, 1703 (1997).

[12] E. J. Brandon, R. D. Rogers, B. M. Burkhart, and Joel S. Miller, Chem.-Eur. J. **4**, 1938 (1998).

[13] Z. Tomkowicz, M. Bałanda, K. Falk, and W. Haase, in *Relaxation Phenomena—Liquid Crystals, Magnetic Systems, Polymers, High-T_c Superconductors, Metallic Glasses*, edited by W. Haase and S. Wróbel (Springer, Berlin, 2003), p. 569.

[14] M. A Gîrțu, C. M. Wynn, K.-I. Sugiura, Joel S. Miller, and A. J. Epstein, J. Appl. Phys. **81**, 1 (1997).

[15] M. A Gîrțu, C. M. Wynn, K.-I. Sugiura, Joel S. Miller, and A. J. Epstein, J. Appl. Phys. **81**, 4410 (1997).

[16] S. J. Etzkorn, W. Hibbs, Joel S. Miller, and A. J. Epstein, Phys. Rev. Lett. **89**, 207201 (2002).

[17] E. J. Brandon, D. K. Rittenberg, A. M. Arif, and Joel S. Miller, Inorg. Chem. **37**, 3376 (1998).

[18] M. Fardis, G. Diamantopoulos, G. Papavassiliou, K. Pokhodnya, Joel S. Miller, and D. K. Rittenberg, and C. Christides, Phys. Rev. B **66**, 064422 (2002).

[19] D. K. Rittenberg and Joel S. Miller, Inorg. Chem. **38**, 4838 (1999).

[20] E. J. Brandon, A. M. Arif, B. M. Burkhart, and Joel S. Miller, Inorg. Chem. **37**, 2792 (1998).

[21] A. D. Adler, F. R. Longo, J. D. Finarelli, J. Goldmacher, J. Assour, and L. Korsakoff, J. Org. Chem. **32**, 476 (1967).

[22] R. D. Jones, D. A. Summerville, and F. Basolo, J. Am. Chem. Soc. **100**, 4416 (1978).

[23] J. Rodríguez-Carvajal, Physica B **192**, 55 (1993).

[24] J. A. Mydosh, *Spin Glasses: An Experimental Introduction* (Taylor and Francis, London, 1993).

[25] D. Hüser, D. J. van Duyneveldt, G. J. Nieuvenhuys, and J. A. Mydosh, J. Phys. C **19**, 3697 (1986).

[26] H. Miyasaka, R. Clérac. K. Mizushima, K. Sugiura, M. Yamashita, W. Wernsdorfer, and C. Coulon, Inorg. Chem. **42**, 8203 (2003).

[27] J. Seiden, J. Phys. (Paris), Lett. **44**, L947 (1983).

[28] K. Nakamura and T. Sasada, Solid State Commun. **21**, 891 (1977); K. Nakamura and T. Sasada, J. Phys. C **11**, 331 (1978).

[29] Y. Imry, P. A. Montano, and D. Hone, Phys. Rev. B **12**, 253 (1975).

[30] C. Coulon, H. Miyasaka, and R. Clérac, Struct. Bonding (Berlin) **122**, 163 (2006).

[31] W. Wernsdorfer, K. Hasselbach, A. Benoit, B. Barbara, B. Doudin, J. Meier, J.-Ph. Ansermet, and D. Mailly, Phys. Rev. B **55**, 11552 (1997); W. Wernsdorfer, B. Doudin, D. Mailly, K. Hasselbach, A. Benoit, J. Meier, J.-Ph. Ansermet, and B. Barbara, Phys. Rev. Lett. **77**, 1873 (1996).

[32] R. J. Glauber, J. Math. Phys. **4**, 294 (1963).

[33] D. P. Goldberg, J. Telser, J. Krzystek, A. G. Montalban, L.-C. Brunel, A. G. M. Barrett, and B. M. Hoffman, J. Am. Chem. Soc. **119**, 8722 (1997).
[34] B. J. Kennedy and K. S. Murray, Inorg. Chem. **24**, 1557 (1985).
[35] D. Hinzke, and U. Nowak, Phys. Rev. B **61**, 6734 (2000).
[36] H.-J. Mikeska and M. Steiner, Adv. Phys. **40**, 191 (1991).
[37] H. B. Braun, J. Appl. Phys. **85**, 6172 (1999).
[38] L. J. de Jongh, C. A. M. Mulder, R. M. Cornelisse, A. J. van Duyneveldt, and J. P. Renard, Phys. Rev. Lett. **47**, 1672 (1981).
[39] H. B. Braun, Phys. Rev. B **50**, 16485 (1994); **50**, 16501 (1994); J. Appl. Phys. **76**, 6310 (1994).
[40] S. S. Eaton, and G. R. Eaton, J. Am. Chem. Soc. **97**, 3660 (1975).
[41] M. Evangelisti, J. Bartolomé, L. J. de Jongh, and G. Filoti, Phys. Rev. B **66**, 144410 (2002).
[42] M. Elmassalami, H. H. A. Smit, H. J. M. de Groot, R. C. Thiel, and L. J. de Jongh, in *Magnetic Excitations and Fluctuations II*, Proceeding in Physics 23, edited by. U. Balacani, S. W. Lovesey, M. G. Rasetti, V. Tognetti (Springer-Verlag, Berlin 1987), p. 178.
[43] F. Ferraro, D. Gatteschi, A. Rettori, and M. Corti, Mol. Phys. **85**, 1037 (1995).